RSC Advances

ROYAL SOCIETY OF CHEMISTRY

www.rsc.org/advances

RSC Advances

ARTICLE

Lignin coating to quench photocatalytic activity of titanium dioxide nanoparticles for potential skincare applications

Received 00th January 20xx,
Accepted 00th January 20xx

DOI: 10.1039/x0xx00000x

www.rsc.org/

M. Morsella,[a] M. Giammatteo,[b] L. Arrizza,[b] L. Tonucci,[c] M. Bressan[a] and N. d'Alessandro[a*]

Ultraviolet light can cause photodamage to the skin, such as sunburn and melanomas. TiO_2 is introduced in sunscreen formulations to reflect and scatter UV radiation. However, it can also photocatalyze the production of reactive species like O^{2-} and $OH^{\cdot}$. Here, we aimed to remove the photocatalytic activity of TiO_2 (anatase and rutile), while preserving the UV filter property. Anatase and rutile were modified through two preparative protocols. The first used HCl lignin precipitation of ethylene glycol lignin solution in the presence of the cross-linker glutaraldehyde and anatase or rutile nanoparticles. The second protocol used HNO_3 lignin precipitation of lignin aqueous solution in the presence of anatase or rutile nanoparticles. Both methodologies were performed at room temperature and ambient pressure in green media, with vigorous mixing followed by 20-kHz sonication. The composite materials obtained were fully characterized by SEM, XRD analysis and FT-IR spectroscopy, and their photostability, and photo and shielding activities were evaluated through reference reactions: oxidation of 2-propanol, an ene-reaction conducted on an α,β-unsaturated carboxylic derivative and photochemical transformation of *o*-nitrobenzaldehyde to *o*-nitrosobenzoic acid. Therefore, in the near future, industrial use of these new clusters can help to minimize TiO_2 phototoxicity in sunscreen formulations, while preserving the sunscreen photoprotection activity.

Introduction

Research in chemistry has always tried to develop different synthesis pathways and to use materials with the lowest possible toxicity levels, in order to generate safer industrial processes. Moreover, eco-friendly and one-pot procedures carried out using innovative products to minimize environmental impact are now being given high priority. For this reason, the use of materials derived from raw plant materials should be favored. This defines the modern concept of sustainability, as was introduced by Anastas and Warner, and as is commonly known as "green chemistry".[1-3]

Photoprotection and its associated risks is an ancient problem that was even carefully considered by our ancestors.[4] The effects of light on the skin can appear immediately or after a long delay. In the first case, there can be reversible damage (erythema), which can be treated pharmacologically. Instead, the effects that typically occur over the long term can be much more dangerous, such as photoaging, immunosuppression, and carcinogenicity.[5-7] Sunscreens[8,9] began to be studied scientifically only from the second half of the last century, and it is well recognized that sunscreens reduce most photodamage to the skin, such as sunburns and melanomas, which are primarily caused by UV radiation.[10-12]

Today, as described in detail in a recent contribution by "L'Oreal Research & Innovation",[13] there is a great need to evaluate the entire sustainability of the productive cycle of a good sunscreen product. The ideal sunscreen should, therefore, provide higher efficacy with broad-spectrum coverage,[14,15] high photostability,[16] good sensorial attributes,[17] and last but not least, at an affordable cost to the consumer. A variety of marketing strategies have led consumers to believe that sunscreen lotions prevent skin damage, while allowing gradual tanning. However, to protect people from serious skin damage, sunscreens must include many more attributes, the most important of which is that the absorbed energy must be dissipated efficiently via photophysical and/or photochemical pathways. This will thus avoid formation of harmful reactive intermediates that can penetrate the skin and be transported into the cells, where they can cause damage to DNA.

Sun filters can be broadly classified into organic absorbers and inorganic particulates.[18-20] All of the available organic filters are of synthetic origin, and they are mainly based on molecules that effectively absorb the UVA and/or UVB radiation.[21] However each group has advantages and disadvantages. For example, cinnamates and diphenylmethanes, have good sunscreen action against both UVA and UVB, but they are either poorly resistant to water (cinnamates) or photounstable (diphenylmethanes), with the formation of by-products that

[a] *Department of Engineering and Geology, University G. d'Annunzio of Chieti-Pescara, Viale Pindaro, 42, 65127 Pescara, Italy.*
Email: dalessan@unich.it; Tel. +3908713555365
[b] *Microscopy Centre, University of L'Aquila, Via Vetoio (Coppito 1), 67100 L'Aquila, Italy.*
[c] *Department of Philosophical, Educational and Economic Science, University G. d'Annunzio, Via dei Vestini, 31, Chieti Scalo, Italy*

† Electronic Supplementary Information (ESI) available: Figures S1-S27; for details of each figure, see the main text. See DOI: 10.1039/x0xx00000x

are not always safe for the skin. Other popular organics have low molar absorbance coefficient in the UVA (e.g., *p*-aminobenzoates, salicylates) or in the UVB region (e.g., benzophenones).[22-24]

Inorganic particulates have been introduced into sunscreen formulations as alternatives or in addition to organic filters, to better reflect, scatter and/or absorb the electromagnetic radiation. Among these inorganic particulates, inert semiconductor metal oxides are the most widely used in commercial sunscreens formulations, such as TiO_2 and ZnO.[25] These metal oxides have bandgaps at ~3 eV, which is within the range of the UV photons in solar light (3.1-4.3 eV), and thus there is a relatively high probability that electron hole pairs are created. There are essentially two such de-excitation mechanisms, as either a simple emission of photon of energy equal to the semiconductor bandgap, or the involvement of the chemical environment of the inorganic particle (i.e., absorbed water, organic moieties). This last can, however, lead to the formation of dangerous species, such as radicals,[26-28] or electrophilic cytotoxic species, such as singlet oxygen.[29,30] Therefore, inorganic filters should be treated before their use in any cosmetic formulations.[31,32] Such treatments might include, for example, coating of the metal oxide core by adding a free radical scavenger (e.g., an antioxidant), or by passivating[33,34] or doping the semiconductor surface with a metal, like vanadium and manganese.[35] Encapsulation technologies have also been used, such as the addition of solid lipid nanoparticles (NPs),[36] zeolites,[37] polymer hybrid nanocapsules,[38] inorganic oxides (which form hydrated oxides that capture hydroxyl radicals; such as SiO_2,[39] ZrO_2 or Al_2O_3),[40] and more recently, graphitized carbon[41] and carbon nanotubes.[42] Alternatively, the addition of antioxidants can minimize the formation of free radicals while still providing protection against UV irradiation, with a preference for antioxidants of natural origin.[43]

Based on these possibilities, we believe that modification of a nanomaterial like TiO_2 using biopolymers would be a good strategy to attain biocompatibility and functionality of the NPs. Lignin is a natural, heterogeneous, phenylpropanoid polymer that is biosynthesized in plants to provide structural rigidity and to prevent the hydrolysis of cellulose, thereby protecting plants from external chemical and/or biological attack.[44] Lignin is currently available in very large quantities as a by-product of the paper and related industries, and its full valorization still represents an important challenge in biorefineries.[45] In this perspective, there are several emerging trends for the use of lignin as feedstock to produce fine chemicals, such as vanillin and other simple monoaromatic derivatives,[46-48] or for new materials to use in industrial catalysis, i.e. nanoaggregates between lignin and metal NPs.[49,50] Moreover, several studies in the medical field have shown that lignin can act as an effective free radical scavenger[51] without inducing irritation to the eyes and skin,[52] thus strongly suggesting that it can be safely used in cosmetic formulations, such as for topical applications.[53]

In the present study, we described two methods for the preparation of TiO_2 NPs coated with lignin, together with their full characterization and a series of tests to evaluate their degree of quenching of the photocatalytic activity of TiO_2.

Experimental Section

Materials

Alkali lignin, ethylene glycol, glutaraldehyde (25% aqueous solution), TiO_2 anatase (nanopowder; particle size, <25 nm), TiO_2 rutile (nanopowder; particle size, <100 nm), *o*-nitrobenzaldehyde (*o*NBA) and tiglic acid (sodium salt) were from Sigma-Aldrich (Italy). Hydrochloric acid (37%), nitric acid (65%), sodium hydroxide pellets and acetone were from Carlo Erba Reagente (Italy). 2-Propanol and 1-butanol were from Fluka (Italy).

Instruments

NMR spectra were recorded using a Bruker Avance 300 spectrometer (7.05 Tesla) equipped with a high-resolution multinuclear probe that was operated in the range of 30 MHz to 300 MHz. The ^1H spectra (^1H NMR) were run in a 5-mm NMR tube that contained a co-axial sealed glass capillary (diameter, 1 mm) that was filled with 30 mM 3-(trimethylsilyl)-2,2,3,3-tetradeutero propionic- acid (sodium salt) in D_2O. The free induction decay was acquired at 22 °C using an appropriate pulse sequence (*zgcppr*; Bruker-made) with a spectral width of -0.5 ppm to 12.5 ppm and with the presaturation signal centered at 4.705 ppm (proton water signal). A 90° excitation pulse (7.6 µs) and a 1-s relaxation delay were used to collect 128 scans for each spectra acquired. The UV visible spectra were recorded using a Jenway 6505 UV/Vis system. Before acquisition, the reaction mixtures were centrifuged and diluted with water, directly into a 3-ml high-precision quartz cell (made of Suprasil® quartz; Hellma), and the spectra were acquired over the wavelength range of 200 nm to 600 nm.

The gas chromatography (GC) apparatus (model 6890; Hewlett Packard) was equipped with a split-splitless injector, a free induction decay detector, and a 5% diphenyl dimethyl polysiloxane capillary column (HP-5 MS; length, 30 m; internal diameter, 0.32 mm; film thickness, 0.25 µm). The acquisition parameters for 2-propanol detection were: injector pressure, 35 kPa; injector temperature, 250 °C; detector temperature, 260 °C; initial temperature, 50 °C (1 min), then 20 °C min^{-1} up to 140 °C (kept for 0 min), and 40 °C min^{-1} up to 250 °C (kept for 5 min). The carrier gas was helium, while 1 µl of the diluted 1:10 solution was injected in split mode (split ratio, 1:15).

For the GC mass spectroscopy (GC-MS) analyses, a gas chromatograph (Thermo Scientific Focus series) was coupled to an ISQ mass-selective detector operated in electron-impact mode at 70 eV. The GC-MS was equipped with a split-splitless injection system and a TR-5 MS (cross-linked, 5% diphenyl dimethyl polysiloxane) capillary column (length, 30 m; internal diameter, 0.25 mm; film thickness, 0.25 µm film thickness) (Thermo Scientific Inc.; Waltham, USA), with helium as the

carrier gas. The acquisition parameters for the detection of volatile derivatives coming from lignin degradation and of *o*NBA were: injections (1 µL) made in split mode (ratio, 1:10); constant injector pressure for all analyses, 20 kPa; injector temperature, 250 °C; source temperature, 250 °C; transfer line temperature, 250 °C; mass range, 33-300 u; initial temperature, 50 °C (1 min), then 10 °C min^{-1} up to 160 °C (kept for 0 min), and 30 °C min^{-1} up to 250 °C (kept for 2.5 min).

A photochemical multiray apparatus (Helios Italquartz; Milano, Italy) was used for photochemical reactions, which contained 10 UV lamps of 15-W power each that emitted light at around 313 nm or 365 nm. Transparent quartz vials (10 mL) were used for irradiation of the suspensions.

The X-ray diffractometer (XRD) analysis was performed on a Miniflex II Rigaku automated power XRD system (Cu Kα radiation, 45 kV, 100 mA) (RINT 2500, Japan). The diffraction data were recorded using continuous scanning at 3° min^{-1}, with 0.010° steps.

The Fourier transform infrared (FT-IR) spectrometer (model 1600; Perkin Elmer) was operated with a spectral window of 4000 cm^{-1} to 400 cm^{-1}.

An ultra-turrax T25 (Janke & Kunkel, IKA Labortechnik, 220 V, 600 W, 50/60 Hz, 24000 min^{-1}) was used for the cluster homogenization. An ultrasonic processor (Model VCX 400; Sonics Ultrasonic Processor; 400 W power, CV 26 Probe; 120 V, 50/60 Hz, 15 amps; probe diameter, 1/8 inch) was used for the cluster sonication. A stereomicroscope (stereozoom S8 APO; Leica) equipped with a camera (EC3) was used to observe the dried powder.

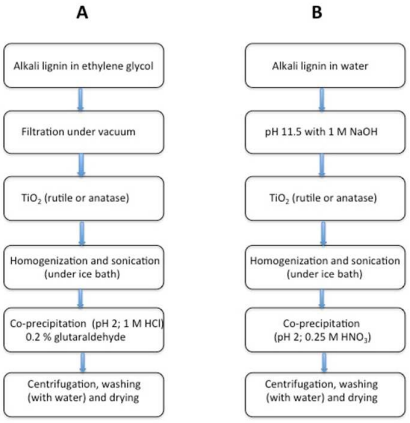

Scheme 1 Detailed protocol adopted for the preparation of the lignin/TiO_2 composite materials.

The transmission electron microscopy images (TEM; CM100; Philips) were obtained using 100 kV as acceleration voltage, and were recorded using a camera (Megaplus, Kodak).

The scanning electron microscopy (SEM) images were performed using a Philips XL30CP equipped with microanalysis (Oxford Inca Energy 250) with both secondary electrons (SE) and back-scatter electrons (BSE) detectors.

Synthesis of TiO_2–lignin clusters

For the syntheses of TiO_2–lignin clusters, we started from the idea developed by Frangville,[54] which precipitated, at acidic pH, the simple lignin NPs, starting from a soluble alkaline lignin. In our study, we added firstly TiO_2 NPs and, after a vigorous homogenization (using an ultraturrax homogenizer), followed by sonication (using an ultrasonic probe operating at 20 kHz), the pH assisted precipitation of the TiO_2-lignin clusters was performed.

In the methodology illustrated in Scheme 1-A, alkali lignin (0.1 g) in ethylene glycol (10 mL) was filtered under reduced pressure (Buchner funnel) to remove insoluble impurities. The stock solution was transferred to a 20-mL test-tube, and TiO_2 powder (0.01 g, anatase/rutile phase) was added. The suspension was stirred for 1 h, homogenized for 2 min, and sonicated for 5 min. The mixture was cooled to 0 °C in an ice bath, and HCl solution (4 ml, 1 M) was added drop-wise. The suspension obtained was again homogenized for 2 min and sonicated for 10 min. After transfer of the entire mixture into a 250-mL flask, aqueous glutaraldehyde solution (0.2% v/v, 30 mL) was added drop-wise under stirring, over 2 h.

In the methodology illustrated in Scheme 1-B, alkali lignin (0.1 g) was added to 7 mL ultrapure water under stirring in a 20-mL test-tube. NaOH (3 mL, 1 M) was added drop-wise, for the lignin solubilisation step. TiO_2 powder (0.01 g, anatase/rutile phase) was added, and the dispersion was homogenized for 4 min, sonicated for 15 min, and cooled in an ice bath. The mixture was diluted with 180 mL ultrapure water, and taken to pH 2 by drop-wise addition of HNO_3 (0.25 M) over 2 h.

In both of these experimental procedures, the lignin/TiO_2 suspensions were centrifuged and the residues (clusters A, B from methodologies in Scheme 1-A, 1-B, respectively) were washed twice with ultrapure water and dried in an oven at 80 °C for 2 h.

Clusters characterization

Following sonication, the samples for TEM analysis were prepared by placing 5 µL of a 10-fold diluted ethanolic solution of the clusters onto 3 mm, 300 mesh, Cu grids (Agar Scientific Ltd).

The powder for SEM analysis was dried, glued onto Al stubs, and then sputter-coated with a thin gold film (20 mA, 45 s). The sample was then embedded in epoxy resin (EpoxiCure™, Buehler), and prior to section analysis, it was polished with polishing cloths with diamond polishing suspensions of decreasing size (9, 3, 1 µm). The SEM analysis of uncoated sections was carried out under low-vacuum conditions.

The samples for XRD analysis were prepared by evaporation of the solvent of an entire cluster suspension, with the resulting powder placed on the glass plate of the instrument.

The samples for FT-IR analysis were prepared by evaporation of the solvent (water) from the cluster suspensions. The resulting residue was milled with KBr (1% w/w) to form a homogeneous powder, which was then compressed into a thin disk that was suitable for the FT-IR analysis.

Stability and photostability studies

Dried clusters were re-suspended in aqueous solutions at room temperature at three different pHs: pH 7 (in phosphate buffer); pH 2 (in 0.01 M HCl); and pH 13 (in 0.1 M NaOH). After 24 h, 8 days, 12 days, 30 days, these samples underwent several analyses (i.e., ^{1}H NMR, GC-MS, UV-vis) to determine the integrity of the clusters through the detection of any short-chain products that can arise from the degradation of lignin. Furthermore, a cluster mixture re-suspended in water was irradiated at 313 nm for 24 h, with the same analyses of their integrity as indicated above, and together with further instrumental analyses, including SEM and IR (data not shown).

Photoactivity

The radical-mediated photooxidation of 2-propanol to acetone[55] (see Scheme 2) was carried out at 313 nm and 365 nm for 48 h. 2-Propanol aqueous solution (10 mL, 5 mM) in a quartz tube and under stirring was irradiated in the presence of a TiO_2 suspension (1 g L^{-1}, anatase/rutile). This was then repeated with the addition of alkali lignin, clusters A and B (of Scheme 1-A and 1-B, respectively), and the lignin/TiO_2 mixture obtained without any treatment, for both anatase and rutile TiO_2. The data were recorded under GC and ^{1}H NMR.

Singlet oxygen photooxidation was determined using the ene reaction performed in the presence of an unsaturated electron-rich derivative (see Scheme 3).[56] A solution of tiglic acid sodium salt in D_2O (10 mM) in a quartz tube (2 mL) was irradiated at 313 nm under stirring for 6 h in the presence of TiO_2 (10 mg, anatase/rutile), to determine the hydroperoxide production (see Scheme 3). Then, this was repeated with the TiO_2 photosensitizer substituted by alkali lignin alone (100 mg), and clusters A and clusters B. The hydroperoxide levels were quantified by ^{1}H NMR.

To test the photoactivities of clusters after the photooxidation of 2-propanol, we removed the solvent by evaporation and we re-suspended the clusters in water; then we carried out again the reaction of photooxidation of 2-propanol under the same condition indicated above.

Shielding activity

The photoconversion of *o*NBA to *o*-nitrosobenzoic acid was used to determine the shielding activity of the prepared samples (see Scheme 4).[57] A methylene chloride solution of *o*NBA (3 mM, 2.5 mL) in a 3-mL spectrophotometric cuvette was irradiated for 1.5 h at 365 nm with a LOT 200 W LSH303/303 27A lamp. The experiment was repeated inserting a further cuvette containing the filters, such as TiO_2 (anatase/rutile), alkali lignin, clusters A or clusters B, between the light source and the cuvette containing the *o*NBA. The residual amounts of reagent were determined by GC-MS analysis.

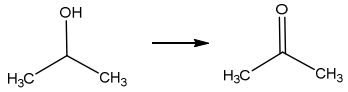

Scheme 2 Photooxidation of 2-propanol. Conditions: TiO_2 suspension in aqueous medium, room temperature, irradiation at 313 and 365 nm.

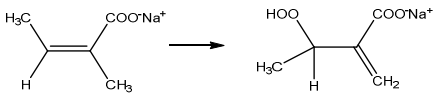

Scheme 3 Ene-reaction between tiglic acid (sodium salt) and singlet oxygen. Conditions: TiO_2 suspension in D_2O, room temperature, aerobic conditions, irradiation at 313 nm.

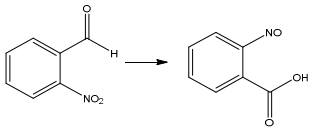

Scheme 4 Photoconversion of *o*-nitrobenzaldehyde to *o*-nitrosobenzoic acid. Conditions: dichloromethane solution, room temperature, irradiation at 365 nm.

Results and Discussion

With the aim being to coat TiO_2 NPs with lignin, we initially realized that simple mechanical mixing of a lignin solution with TiO_2 particles, will not generate a homogeneous coating, even under various experimental conditions. This is because TiO_2 quickly aggregates and separates out as a white solid at the bottom of the lignin-containing solution.

Therefore, to make effective an "interaction" between lignin and TiO_2, a precipitation method needs to be used. Our method consists of precipitation of lignin at appropriate pHs (i.e., from alkaline to neutral-acidic) in presence of nano-TiO_2; furthermore, the possible presence of a crosslinker (i.e., glutaraldehyde) was taken into consideration.

Several commercially available lignins were initially taken into consideration, but only alkaline lignin, which is soluble at pH > 11, gave encouraging results in terms of lignin precipitation on the titania particle surface as lignin/TiO_2 clusters. We applied this methodology to lignin solutions containing TiO_2 suspensions, either in ethylene glycol in the presence of glutaraldehyde cross-linker (Scheme 1-A) or in alkaline water (without glutaraldehyde; Scheme 1-B).

The detailed pathways are illustrated in Scheme 1. Comparing these two synthetic procedures, we noted that the initial dark brown color of the solutions (which was more intense for the aqueous solution; see Fig. S1 in the ESI) turned dark green when following Scheme 1-A, likely due to cross-polymerization of the crosslinking agent with lignin,[58] and turned yellow-orange when following Scheme 1-B. Fig. S2-S5 in the ESI show light microscope images of the obtained materials. To achieve a good mixing and to reduce the particles size of the composite material, vortex homogenization was used, followed by ultrasonic treatment (20 kHz).[59] Phase separation was never observed, even after ultracentrifugation.

Characterization

The characterization of the TiO_2-lignin clusters particles was performed by IR spectroscopy, XRD analysis and TEM and SEM. The IR spectra showed a clear-cut change in the shape of the broad band in the 500-800 cm^{-1} region, where the Ti-O-Ti vibration is expected to fall (Fig. 1 and Fig. S6). This indicates a modification of the structure of the inorganic moiety, likely due to a strong interaction with the organic part of composite. Moreover, in Scheme 1-B, where the strong oxidant HNO_3 used induced a partial bleaching of the lignin, the resulting yellow-orange materials showed new absorption peaks in the IR spectra. Those at 2940, 2361, 1722, 1631 and 1384 cm^{-1} were attributable to the oxidized (carbonyl) forms of the alcoholic moieties of lignin, and those at 1545 and 1339 cm^{-1} were attributable to nitro groups introduced in the lignin skeleton.

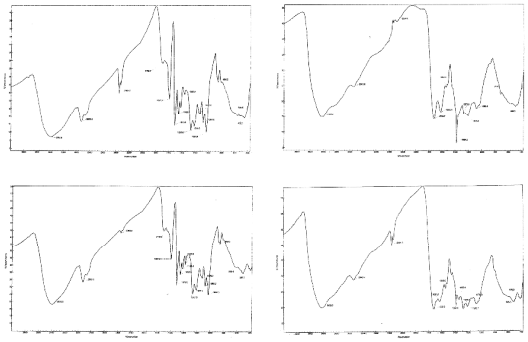

Figure 1 Representative IR spectra of clusters A (left) and B (right) for anatase (top) and rutile (bottom).

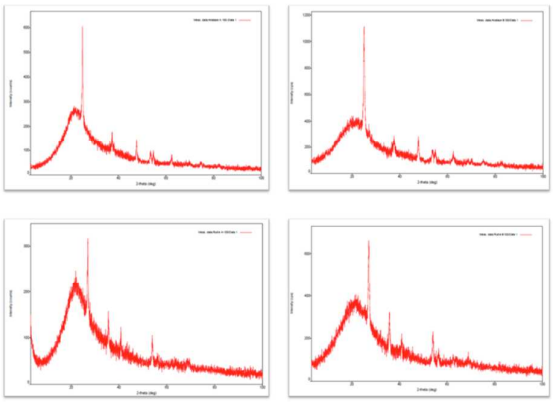

Figure 2 Representative XRD analyses of clusters A (left) and B (right) for anatase (top) and rutile (bottom).

The XRD analyses showed that the initial crystalline phase of TiO_2 were preserved under these treatments, whereas no other solid crystalline by-products were detected (Fig. 2, Fig. S7 and S8 in the ESI). We applied the Sheerer formula to determine the sizes of the particles, although not successfully, possibly due to their irregular shapes (i.e., nonspherical), as also demonstrated by SEM analysis (see below).

Preliminary screening was carried out using light microscopy and TEM. In the TiO_2 samples of both anatase and rutile the particles were nanometer size (20-40 nm for anatase and 80 100 nm for rutile), with a tendency to aggregation (see Fig. S9-S12 in the ESI). In contrast, with lignin alone (see Fig. S13 in the ESI) or in association with TiO_2 (see Fig. S14 and S15 in the ESI), the images were difficult to interpret, likely because of to the thickness of the particles, too large to be resolved with any accuracy.

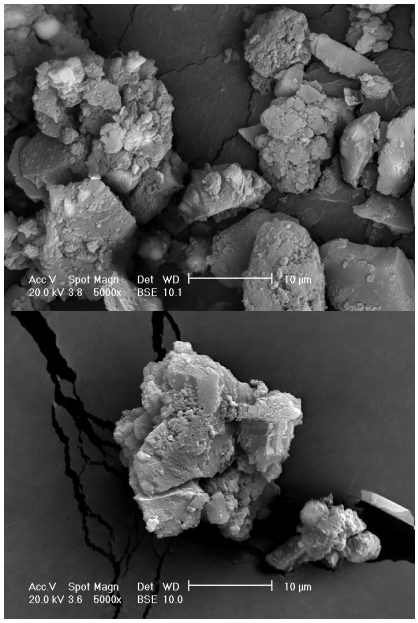

Figure 3 Representative SEM images of cluster A containing anatase (top) and rutile (bottom) (5000x of magnification)

The SEM images of TiO_2 alone (Fig. S16), by confirming the data acquired by TEM, allowed the resolution of the structure of the lignin, which was seen as empty spherical particles that were micrometer size (50-100 µm; Fig. S17). The TiO_2-lignin cluster particles had irregular shapes, irrespective of the preparative method used: they exhibited a powdery aspect when containing anatase TiO_2, while with rutile TiO_2 were more angular. In all cases, these particles were strongly reduced in size (to 10-20 µm) with respect to pure lignin and showed a tendency to aggregate that was comparable to that of the naked TiO_2 particles (Fig. 3 and 4; Fig. S18-S21). Indeed, the ultrasound treatment, in favouring the reduction of the sizes of lignin particles, also prevented aggregation of the TiO_2

NPs, which appeared to be homogeneously dispersed inside the lignin matrix. All samples were polished and then examined again by SEM. The polished samples images showed high dispersion of the TiO_2 NPs, with marked differences between anatase and rutile TiO_2. The anatase NPs, apparently because of their smaller sizes, showed higher aggregation than the rutile NPs and always appeared as white agglomerates dispersed inside the lignin matrix; in contrast, rutile nanoparticles looked like a homogeneously dispersed fine powder that was difficult to see at low magnification. In short, the visual impression of these SEM images (Fig. 5 and 6; Fig. S22-S25) resembled "dark chocolate cake" (i.e., the lignin) that contains "white chocolate chips" (i.e., the TiO_2) for the anatase samples, or "coconut flour" (i.e., the TiO_2) for the rutile ones. Microanalyses, carried out on the particles (see Fig. S26-S29 in the ESI) or on their sections (see Fig. S30-S33 in the ESI), confirmed the presence of the expected elements, i.e. carbon, titanium and oxygen.

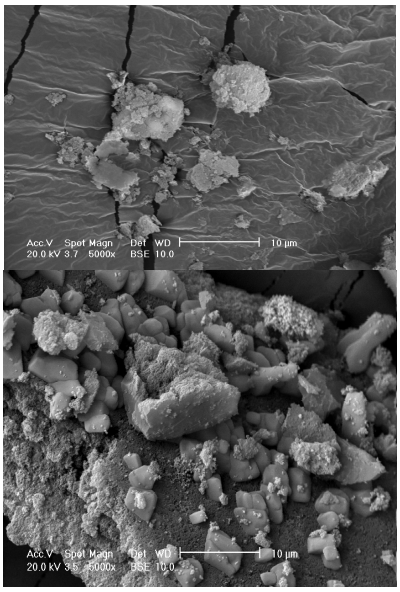

Figure 4 Representative SEM images of cluster B containing anatase (top) and rutile (bottom) (5000x of magnification)

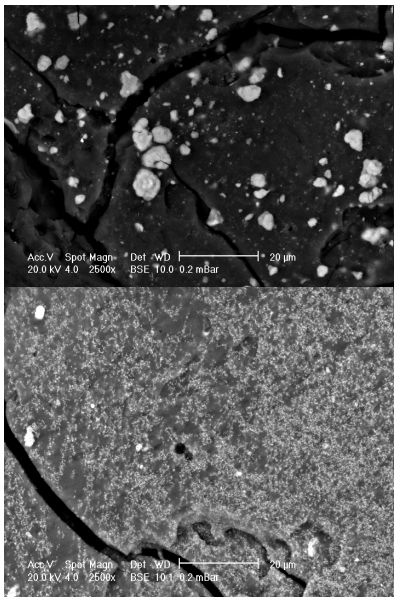

Figure 5. Representative SEM images of polished sample of cluster A with anatase (top) and rutile (bottom) (2500x of magnification)

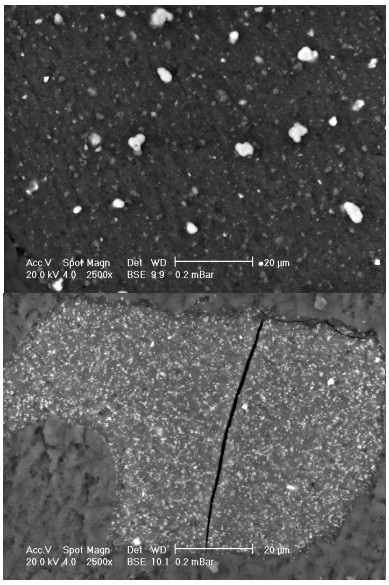

Figure 6. Rappresentative SEM images of polished sample of cluster B with anatase (top) and rutile (bottom) (2500x of magnification)

Stability and photostability studies

Tests of the stabilities of the composite materials were performed for water suspensions, at acidic, neutral and alkaline pHs. The presence in the supernatant of short chain products that came from lignin degradation/modification (e.g., methanol, formic acid, acetic acid, vanillin, among others) was used to determine the stability/photostability of the materials, and also the potential quenching role of lignin as a sacrificial protector.

Even after 30 days in the dark no degradation products were detected for the A clusters under any of the experimental conditions used; the IR spectra were superimposable to those of the initial clusters. Instead, in the same conditions, the supernatant of the materials obtained by following Scheme 1-B, always turned light yellow, while containing small amounts of degradation products (i.e., methanol, formic acid, vanillin), more abundant at higher pH, in agreement with a previous report on lignin nanoparticles.[54]

When the neutral water suspension of the clusters was irradiated at 313 nm for 24 hours, both the SEM images and the IR spectra remained unchanged. For the Scheme 1-A clusters, the supernatant remained always colourless, although containing small amounts of methanol, while the Scheme 1-B clusters resulted in a light yellow water phase, with formation of methanol, formic acid, vanillin and acetic acid to greater levels than those formed in the dark (see Fig. S34 and S35 in the ESI).

Photoactivity

The photoactivity was evaluated using two reference reactions: the photooxidation of 2-propanol to acetone[55] and the ene-reaction between the TiO_2-photogenerated singlet oxygen and tiglic acid (a standard electron-rich unsaturated model derivative, which yields, as dominant reaction product, 2-carboxy-3-hydroperoxo-1-butene).[56]

Once it had been ascertained by ^{1}H NMR that TiO_2 does not physically retain the alcohol, an aqueous solution of 2-propanol (5 mM) was irradiated under stirring at both 313 and 365 nm for 48 h in the presence of the materials under examination. As shown by the time course for the irradiation at 313 nm in Fig. S36 in the ESI (the data for irradiation at 365 nm were comparable; data not shown), 2-propanol remained substantially unchanged (within a 10% approximation) in the presence of the four examined clusters (i.e., for anatase and rutile, and under Scheme 1-A and 1-B), all of which clearly acting as inhibitors of the phooxidation reaction (Fig. 7). On the contrary, the reaction mixtures containing anatase or rutile alone showed, as expected, strong photocatalytic activity (by being anatase more effective than rutile). Finally, for a mechanical mixture of lignin and TiO_2, only 45% of 2-propanol remained unreacted upon irradiation, pointing to a partial quenching of the photocatalytic activity.

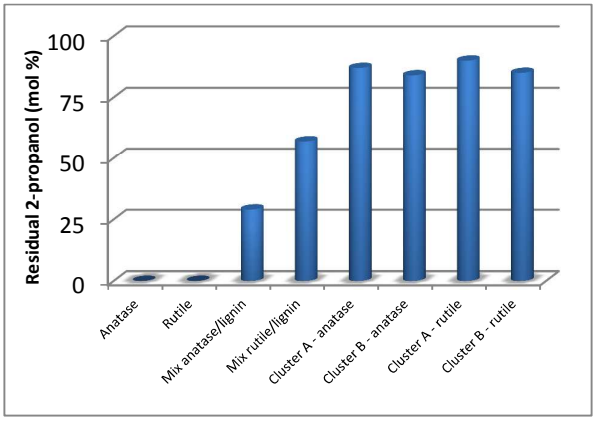

Figure 7. Quantification of residual 2-propanol after photooxidation under 48 h of irradiation at 310 nm for TiO_2 alone and with lignin, and for the clusters A and B (according to Scheme 1) for anatase and rutile TiO_2, as indicated. Values are mean of three replicates; percent errors are always < 10%

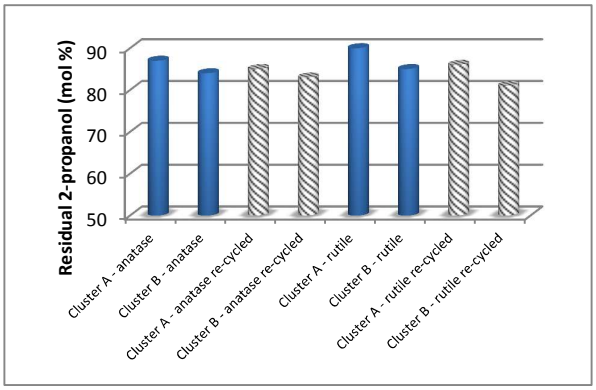

Figure 8. Quantification as for Figure 7, and when the clusters were re-cycled a second time, as indicated. Values are mean of three replicates; percent errors are always < 10%

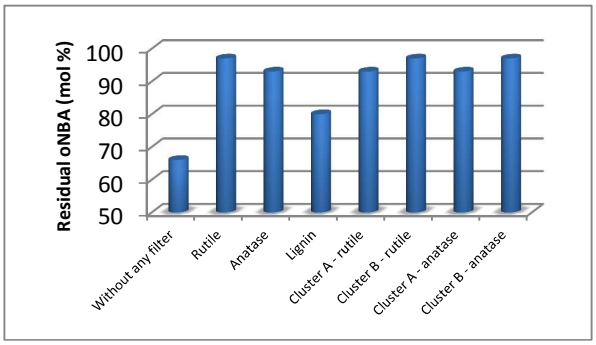

Figure 9. Quantification of residual *o*NBA after 1.5 h irradiation at 365 nm, without any filter, and with filters of TiO_2 alone and with lignin, and for the clusters A and B (according to Scheme 1) for anatase and rutile TiO_2, as indicated. Values are mean of three replicates; percent errors are always < 10%

Of note, the crosslinking agent appears to be critical for the stabilization of the composite material, especially when in the alkaline media, while it does not have a role in the quenching of the photocatalytic activity of TiO_2. Finally here, and as shown in Fig. 8, comparable percentages of residual 2-propanol were seen when neo-synthetized or re-cycled clusters were used, for both anatase and rutile TiO_2 phases.

When tiglic acid (sodium salt) in D_2O (10 mM) was irradiated at 313 nm in the presence of the various samples, small amounts of the expected 2-carboxy-3-hydroperoxo-1-butene were detected only with anatase and rutile TiO_2 alone (10 % and 4 % conversions, respectively, after 6 h). With lignin and with the clusters following Scheme 1-A and 1-B, no reaction was observed, thus indicating that singlet oxygen was not formed, or, if formed, in very small amounts, not of concern for significant oxidative effects (see Fig. S37 of the ESI).

Shielding activity

The photo-protection activity was determined according to the photoconversion of *o*NBA to *o*-nitrosobenzoic acid.[57] This was achieved by irradiation of a quartz cuvette containing 3 mM *o*NBA in dichloromethane, using a UV lamp (200 W) at 365 nm. This test was repeated in the presence of filters, which were put into a second cuvette placed between the irradiation source and an *o*NBA sample. After 1.5 h irradiation, 34% of the *o*NBA was converted in the absence of any filters (Fig. 9), whereas with the alkali lignin filter, lower conversion was observed (20%), likely because of the relatively low UV absorption by the lignin (see Fig. S38 of the ESI). In contrast, in the presence of the TiO_2 (both anatase and rutile) suspensions as filters, *o*NBA was almost completely preserved (indeed, TiO_2 is a well known inorganic filter that effectively reflects UV radiation) and exactly the same result was observed with the clusters Scheme 1-A and 1-B as filters, for both the anatase and rutile TiO_2. Therefore, and notwithstanding the micrometric size of the particles, photoprotection by these clusters was more effective than lignin, by reaching the same level of the naked TiO_2.

Conclusions

A simple and versatile procedure that can be used to prepare TiO_2-lignin composite materials was developed here. The experimental conditions adopted were mild and the by-products from the overall procedure (i.e., ethylene glycol, glutaraldehyde) were soluble in water, and were thus removable by simple water washing. After the full characterization of the clusters from Scheme 1-A and 1-B, we evaluated their photochemical properties. All the examined clusters induced almost complete quenching of the photocatalytic power of TiO_2 and complete inhibition of the production of singlet oxygen by TiO_2 (when used under aerobic conditions), whereas they retained the same photoprotection activity as TiO_2. We can assume here that the UV photons can be absorbed by both lignin and TiO_2, but when TiO_2 is activated, the lignin layer helps to dissipate the photogenerated electrons, which appears to occur via sacrificial chemical reactions that lead to the formation of short chain molecules.

As the sizes of these particles are important for the acceptability of the cosmetic preparation (i.e., smaller particles in the formulation will result in a more homogeneous and natural skin color), a further evolution of this study can be envisaged, with the aim to reduce the size of the particles. Other improvements can be achieved by investigating other crosslinkers, which should include in particular those of natural origin, like genipin[60] or olive leaf extract.[61]

A small amount of inorganic sunscreen is required in the cosmetic formulations, therefore the dark colour of lignin should not be a problem. Anyway, modifying the lignin structure by simple oxidation reactions, it is possible to bleach partially the polymer overcoming this potential problem. Moreover, the light brown colour might be used in other daily cosmetics (e.g., the last novelty of cosmetics called BB Cream - Blemish Balm Cream) to protect and to donate a light colour to the skin.

Finally, it would be intriguing to combine physical and chemical photoprotection by functionalizing the lignin with a common organic sunscreen chromophores.

Conflicts of interest

The author declares no conflict of interest.

Author Contributions

The manuscript was written through contributions of all authors. All authors have given approval to the final version of the manuscript.

Abbreviations

NPs	nanoparticles;
GC	gaschromatograph
GC-MS	gas chromatograph mass spectrometry
XRD	X-ray diffractometry
NMR	nuclear magnetic resonance

Aknowledgements

We thank the “Consorzio di Ricerca per l’Innovazione Tecnologica, la Qualità e la Sicurezza degli Alimenti S.C.R.L.” (CIPE funding 20.12.04; DM 28497) and the “Ministero dell’Istruzione, dell’Università e della Ricerca” (MIUR) for financial support. MM thanks the “Scuola Superiore” of the ‘G. d’Annunzio’ University for the scholarship relative to the PhD programme (cycle XXVIII).

Notes and references

1 P. T. Anastas and J. C. Warner, *Green chemistry: theory and practice*, Oxford University Press, New York, USA, 2000.

2 R. A. Sheldon, *Green Chem.,* 2014, **16**, 950.
3 C. O. Tuck, E. Pérez, I. T. Horváth, R. A. Sheldon and M. Poliakoff, *Science,* 2012, **337**, 695.
4 J. M. Goulart and S. Q. Wang, *Photochem. Photobiol. Sci.,* 2012, **9**, 432.
5 O. N. Agbai, K. Buster, M. Sanchez, C. Hernandez, R. V. Kundu, M. Chiu, W. E. Roberts, Z. D. Draelos, R. Bhushan, S. C. Taylor and H. W. Lim, *J. Am. Acad. Dermatol.,* 2014, **70**, 748.
6 D. A. Lazovich, R.I. Vogel, M. Berwick, M. A. Weinstock, E. M. Warshaw and K. E. Anderson, *Cancer Epidemiol. Biomarkers Prev.,* 2011, **20**, 2583.
7 E. Dupont, J. Gomez and D. Bilodeau, *Int. J. Cosmetic Sci.,* 2013, **35**, 224.
8 J. Krutmann, A. Morita and J. H. Chung, *J. Invest. Dermatol.,* 2012, **132**, 976.
9 D. R. Sambandan and D. Ratner, *J. Am. Acad. Dermatol.,* 2011, **64**, 748.
10 P. C. Jou, R. J. Feldman and K. J. Tomecki, *Clev. Clin. J. Med.,* 2012, **79**, 427.
11 A. Fourtanier, D. Moyal and S. Seite, *Photochem. Photobiol. Sci.,* 2012, **11**, 81.
12 M. E. Burnett and S. Q. Wang, *Photodermatol. Photoimmunol. Photomed.,* 2011, **27**, 58.
13 M. Philippe, B. Didillon and L. Gilbert, *Green Chem.,* 2012, **14**, 952.
14 P. Schroeder and J. Krutmann, *Skin Theraphy Lett.,* 2010, **15**, 4.
15 U. Osterwalder and B. Herzog, *Photochem. Photobiol. Sci.,* 2010, **9**, 470.
16 E. Damiani, P. Astolfi, J. Giesinger, T. Ehlis, B. Herzog, L. Greci and W. Baschong, *Free Rad. Res.,* 2009, 1.
17 U. Osterwalder, M. Sohn and B. Herzog, *Photodermatol. Photoimmunol. Photomed.,* 2014, **30**, 62.
18 N. A. Shaath, *Photochem. Photobiol. Sci.,* 2010, **9**, 464.
19 M. S. Latha, J. Martis, V. Shobha, R. S. Shinde, S. Bangera, B. Krishnankutty, S. Bellary, S. Varughese, P. Rao and N. Kumar, *J. Clin. Aesthetic Dermatol.,* 2013, **6**, 16.
20 N. Serpone, D. Dondi and A. Albini, *Inorg. Chim. Acta,* 2007, **360**, 794.
21 R. Jansen, U. Osterwalder, S. Q. Wang, M. Burnett and H. W. Lim, *J. Am. Acad. Dermatol.,* 2013, **69**, 867.e1-867.e14.
22 M. N. Chrétien, L. Migahed and J. C. Scaiano, *Photochem. Photobiol.,* 2006, **82**, 1606.
23 F. Brugè, L. Tiano, P. Astolfi, M. Emanuelli and E. Damiani, *Plos One,* 2014, **9**, 1.
24 D. Dondi, A. Albini and N. Serpone, *Photochem. Photobiol. Sci.,* 2006, **5**, 835.
25 T. G. Smijs and S. Pavel, *Nanotechnol. Sci. Appl.,* 2011, **4**, 95.
26 R. Dunford, A. Salinaro, L. Cai, N. Serpone, S. Horikoshi, H. Hidaka and J. Knowland, *FEBS Lett.,* 1997, **418**, 87.
27 G. Wakefield, M. Green, S. Lipscomb and B. Flutter, *Mater. Sci. Technol.,* 2004, **20**, 985.
28 Z. Pan, W. Lee, L. Slutsky, R. A. F. Clark, N. Pernodet and M. H. Rafailovich, *Small,* 2009, **5**, 511.
29 M. Buchalska, G. Kras, M. Oszajca, W. Lasocha and W. J. Macyk, *Photochem. Photobiol. A,* 2010, **213**, 158.
30 I. Fenoglio, J. Ponti, E. Alloa, M. Ghiazza, I. Corazzari, R. Capomaccio, D. Rembges, S. Oliaro-Bosso and F. Rosi, *Nanoscale,* 2013, **5**, 6567.
31 M. N. Chrétien, E. Heafey and J. C. Scaiano, *Photochem. Photobiol.,* 2010, **86**, 153.
32 W. Macyk, K. Szacilowski, G. Stochel, M. Buchalska, J. Kuncewicz and P. Labuz, *Coord. Chem. Rev.,* 2010, **254**, 2687.
33 N. Serpone, A. M. Salinaro, S. Horikoshi and H. Hidaka, *J. Photochem. Photobiol. A,* 2006, **179**, 200.
34 I. Corazzari, S. Livraghi, S. Ferrero, E. Giamello, B. Fubini and I. Fenoglio, *J. Mater. Chem.,* 2012, **22**, 19105.
35 G. Wakefield, S. Lipscomb, E. Holland and J. Knowland, *Photochem. Photobiol. Sci.,* 2004, **3**, 648.
36 D. Nesseem, *Int. J. Cosmetic Sci.,* 2011, **33**, 70.
37 B. Shen and J. C. Scaiano, A. M. English, *Photochem. Photobiol.,* 2006, **82**, 5.
38 J. Xiao, W. Chen, F. Wang and J. Du, *Macromolecules,* 2013, **46**, 375.
39 A. Jaroenworaluck, N. Pijarn, N. Kosachan and R. Stevens, *Chem. Eng. J.,* 2012, **181-182**, 45.
40 T. Picatonotto, D. Vione and M. E. Carlotti, *J. Dispersion Sci. Technol.,* 2002, **23**, 845.
41 A. Vuorema, J. J. Walsh, M. Sillanpaa, W. Thielemans, R. J. Forster and F. Marken, *Electrochim. Acta,* 2012, **73**, 31.
42 W. Sukchom, K. Chayantrakom, P. Satiracoo and D. Baowan, *J. Nanomaterials*, 2011, Article ID 857864, 8 pages.
43 W. A. Lee, N. Pernodet, B. Li, C. H. Lin, E. Hatchwell and M. H. Rafailovich, *Chem. Commun.,* 2007, 4815.
44 F. G. Calvo-Flores and J. A. Dobado, *Chem. Sus. Chem.,* 2010, **3**, 1227.
45 S. Dutta, K. C. W. Wu and B. Saha, *Catal. Sci. Technol.,* 2014, **4**, 3785.
46 H. Priefert, J. Rabenhorst and A. Steinbüchel, *Appl. Microbiol. Biotechnol.,* 2001, **56**, 296.
47 J. Zakzeski, P. C. A. Bruijnincx, A. L. Jongerius and B. M. Weckhuysen, *Chem. Rev.,* 2010, **110**, 3552.
48 L. Tonucci, F. Coccia, M. Bressan and N. d'Alessandro, *Waste Biomass Valoriz.,* 2012, **3**, 165.
49 F. Coccia, L. Tonucci, D. Bosco, M. Bressan and N. d'Alessandro, *Green Chem.,* 2012, **14**, 1073.
50 F. Coccia, L. Tonucci, P. D'Ambrosio, M. Bressan and N. d'Alessandro, *Inorg. Chim. Acta,* 2013, **399**, 12.
51 T. Dizhbite, G. Telysheva, V. Jurkjane and U. Viesturs, *Bioresource Technol.,* 2004, **95**, 309.
52 M. P. Vinardell, V. Ugartondo and M. Mitjans, *Ind. Crops Prod.,* 2008, **27**, 220.
53 Y. Qian, X. Qiu and S. Zhu, *Green Chem.,* 2015, **17**, 320.
54 C. Frangville, M. Rutkevicius, A. P. Richter, O. D. Velev, S. D. Stoyanov and V. N. Paunov, *Chem. Phys. Chem.,* 2012, **13**, 4235.
55 F. J. Lopez-Tenllado, A. Marinas, F. J. Urbano, J. C. Colmenares, M. C. Hidalgo, J. M. Marinas and J. M. Moreno, *Applied Catal. B: Environment.,* 2012, **128**, 150.
56 P. D'Ambrosio, L. Tonucci, N. d'Alessandro, A. Morvillo, S. Sortino and M. Bressan, *Eur. J. Inorg. Chem.,* 2011, 503.
57 K. L. Willett and R. A. Hites, *J. Chem. Educat.,* 2000, **77**, 900.
58 I. Migneault, C. Dartiguenave, M. J. Bertrand and K. C. Waldron, *Biotechniques,* 2004, **37**, 790.
59 I. A. Gilca, V. I. Popa and C. Crestini, *Ultrasonics Sonochemistry,* 2015, **23**, 369.
60 H. Hezaveh and I. I. Muhamad, *Korean J. Chem. Eng.,* 2012, **29**, 1647.
61 I. Erdogan, M. Demir and O. Bayraktar, *J. Appl. Polymer Sci.,* 2015, DOI: 10.1002/APP.41338.